

OPTICAL AND X-RAY CLUSTERS AS TRACERS OF THE SUPERCLUSTER-VOID NETWORK. II THE SPATIAL CORRELATION FUNCTION

E. TAGO¹, J. EINASTO¹, M. EINASTO¹, V. MÜLLER² & H. ANDERNACH³

Draft version October 29, 2018

ABSTRACT

We study the space distribution of Abell and X-ray selected clusters of galaxies from the ROSAT Bright Source Catalog, and determine correlation functions for both cluster samples. On small scales the correlation functions depend on the cluster environment: clusters in rich superclusters have a larger correlation length and amplitude than all clusters. On large scales correlation functions depend on the distribution of superclusters. On these scales correlation functions for both X-ray and Abell clusters are oscillating with a period of $\sim 115 h^{-1}$ Mpc. This property shows the presence of a dominating scale in the distribution of rich superclusters.

Subject headings: cosmology: large-scale structure of the universe – cosmology: observations – galaxies: X-ray clusters

1. INTRODUCTION

The distribution of matter can be characterized by the power spectrum, the correlation function, the void probability function, and other suitable distribution functions. On scales up to about $100 - 200 h^{-1}$ Mpc (in this paper we denote Hubble constant as $H_0 = 100 h \text{ km s}^{-1} \text{ Mpc}^{-1}$) the power spectrum of galaxies and clusters of galaxies has been determined in a number of studies using available surveys; for recent reviews about the power spectrum see Peacock & Dodds (1994), Vogeley (1998), Einasto et al. (1999a, hereafter E99a), Retzlaff (1999), Schuecker et al. 2000, and Miller and Batuski (2000). These studies show that on smaller scales the power spectrum exhibits an almost exact power law of index $n \simeq -1.9$, has a maximum at $k \simeq 0.05 \pm 0.01 h \text{ Mpc}^{-1}$, or wavelength $\lambda \approx 120 h^{-1}$ Mpc, and probably approaches the Harrison-Zeldovich spectrum with power index $n = 1$ on very large scales. The exact shape of the power spectrum around the maximum and beyond is known with rather low accuracy. Einasto et al. (1997a) and Retzlaff et al. (1998) find that the power spectrum of Abell clusters has a sharp peak near $k = 0.05$, whereas Miller & Batuski (2000) did not detect a strong feature on this scale.

Another popular method to characterize the large-scale structure is the use of the correlation function; for recent studies, including on X-ray sources, see Romer et al. (1994), Einasto et al. (1997b, hereafter E97b), Guzzo (1999), Abadi et al. (1998), Lee & Park (1999), Guzzo et al. (1999), Tesch et al. (2000), Moscardini et al. (2000a,b) and Collins et al. (2000). In most studies the correlation function has been investigated only in a relatively small distance range up to about $100 h^{-1}$ Mpc. In these studies a log-log representation was used, thus it was possible to investigate the function only in the range of separations where the correlation function is positive. On larger scales, using a non-logarithmic representation, E97b and Broadhurst & Jaffe (1999) found oscillations of the spatial correlation function. Oscillations are manifested by alternating peaks and valleys

of the functions with a period of $\approx 120 h^{-1}$ Mpc.

The primary goal of the present paper is to compare the distribution of optically selected Abell (1958), and Abell, Corwin & Olowin (1989) clusters with the distribution of X-ray selected clusters. Of particular interest is the comparison of distributions on large scales and to check the presence of a preferred scale around $120 h^{-1}$ Mpc. We shall use the correlation function analysis as this function is more sensitive to the presence of the regularity in the distribution of clusters (E97b).

The ROSAT all-sky X-ray imaging survey has provided a unique possibility to compile samples of clusters independently of the previous optical catalogs. There exist several cluster surveys based on ROSAT observations: the ROSAT-ESO Flux Limited X-ray (REFLEX) cluster survey (Guzzo et al. 1999, Collins et al. 2000, Schuecker et al. 2000), the ROSAT Brightest Cluster Sample (BCS, Ebeling et al. 1998, 2000), the RASS1 Bright Sample southern survey (De Grandi et al. 1999), and the ROSAT Bright Survey (RBS, Schwöpe et al. 2000); the latter is based on the ROSAT all-sky Bright Source Catalog (RBSC, Voges et al. 1999). We shall use the sample of X-ray clusters by Schwöpe et al. (2000) since this is the only available all-sky survey of X-ray selected clusters so far. Redshifts are presently available for almost all objects in this catalog. We use a new version of the compilation of redshifts of Abell clusters to study the distribution of X-ray selected clusters in superclusters determined by Abell clusters (Einasto et al. 2001a, Paper I).

The paper is organized as follows. In the next Section we shall describe X-ray and optically selected samples of clusters of galaxies used in the study. In Section 3 we shall determine relevant selection functions and calculate the correlation functions for X-ray and Abell clusters. Here we determine the correlation function for all clusters of Abell and X-ray selected samples, as well as correlation functions of clusters located in superclusters. Lists of clusters in superclusters were published in Paper I. In Section 4 we present

¹Tartu Observatory, EE-61602 Tõravere, Estonia

²Astrophysical Institute Potsdam, An der Sternwarte 16, D-14482 Potsdam, Germany

³Depto. de Astronomía, Univ. Guanajuato, Apdo. Postal 144, Guanajuato, C.P. 36000, GTO, Mexico

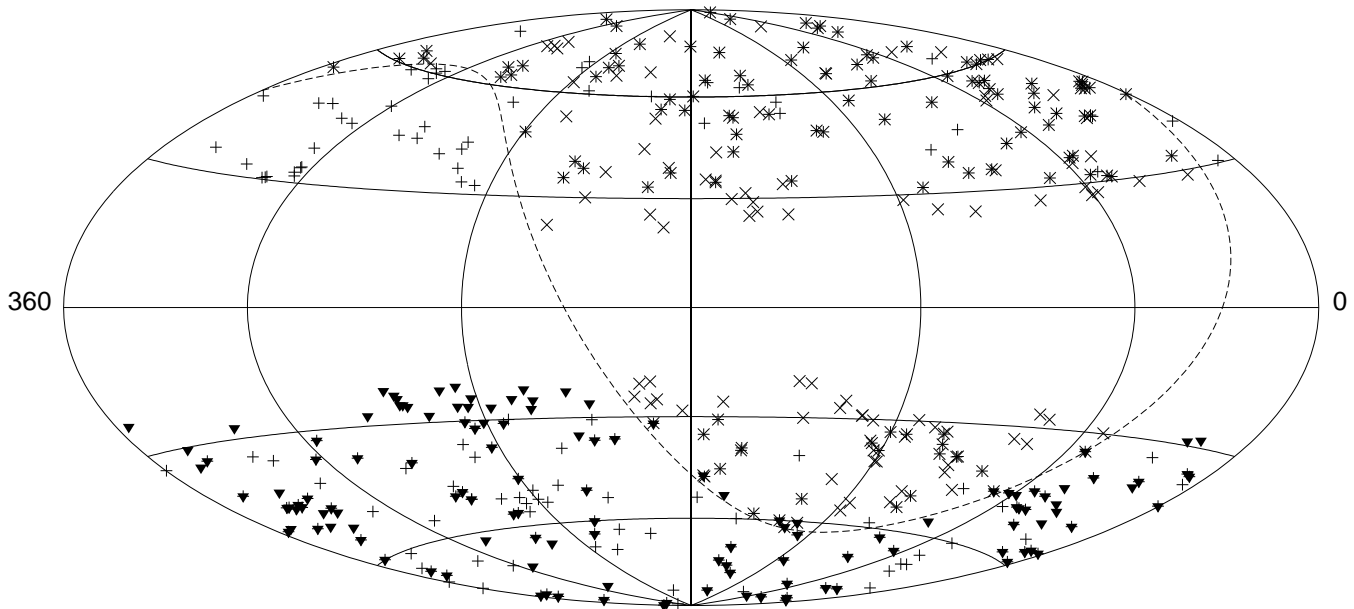


FIG. 1.— Sky coverage presented in Galactic coordinates for three X-ray selected clusters samples: + for Schwope et al. (RBS), x for Ebeling et al. (RASS BCS), and triangles for De Grandi et al. (RASS1 Bright Sample). Asterisks appear when clusters from the two first samples coincide. The dashed line denotes the celestial equator (declination $\delta = 0^\circ$).

the analysis of the nearest neighbor distribution for X-ray cluster systems, and in Section 5 we briefly discuss our results and give conclusions.

2. DATA

2.1. X-ray selected samples

ROSAT observations were made with the Position Sensitive Proportional Counter in the broad (0.1 – 2.4 keV), soft (0.1 – 0.4 keV) and hard energy band (0.5 – 2.0 keV) (Voges et al. 1999). The ROSAT All-Sky Survey Bright Source Catalog (RASS-BSC) contains in total 18,811 sources down to a limiting count rate 0.05 cts/s. Presently three surveys of X-ray selected clusters of galaxies based on ROSAT observations are available, those by Ebeling et al. (1998, 2000), De Grandi et al. (1999), and Schwope et al. (2000). In this paper we use the ROSAT Bright Survey (RBS, Schwope et al. 2000). This catalog of all high-Galactic latitude RASS sources with PSPC count-rate above 0.2 s^{-1} contains a total of 302 X-ray clusters and is the only available survey covering the whole sky (excluding the zone of avoidance). We denote this cluster sample as the “RBS” sample.

Figure 1 shows the sky distribution of clusters for these samples. Here we can compare the sample selection criteria and the sky coverage for these catalog to estimate the best sample for our purposes. Table 1 presents some parameters for these samples. We see that the RBS sample is the only one that covers both hemispheres, although a wider zone of avoidance has been used – an advantage to reduce latitude selection effects.

We have used a restricted sub-sample of the RBS catalog. Figure 2 (left-hand panel) presents the X-ray luminos-

ity versus distance distribution for the RBS cluster sample. As in Paper I all distances have been calculated using the formula by Mattig (1958). The sharp edge at the lower part of the distribution corresponds to the survey flux (apparent X-ray magnitude) limit. For the calculation of the correlation function and multiplicity function we have restricted our sample to limit of X-ray *absolute luminosity* $L_x \geq 10^{43} \text{ erg/s}$. Up to the distance where this luminosity equals the flux limit used (approximately $100 h^{-1} \text{ Mpc}$), our sample is volume limited. At larger distances the sample is flux limited, and thus subject to a bias similar to the Malmquist bias in optically selected galaxy catalogs. Due to this effect the sample becomes very diluted on large scales. To decrease the influence of this effect we have cut the sample at a distance of $250 h^{-1} \text{ Mpc}$. Our previous experience has shown that very diluted samples do not represent well the distribution of high-density regions in the universe (E97b). The mentioned restriction in luminosity and distance provided a more homogeneous sample of 137 X-ray clusters which we shall refer to as the “RBS.250” sample.

2.2. Abell cluster samples

For comparison with X-ray clusters we shall study the clustering properties of optically selected Abell clusters of galaxies (Abell 1958, Abell, Corwin & Olowin 1989). Here we use the March 1999 version of the redshift compilation for Abell clusters described by Andernach & Tago (1998). This sample was described in Paper I. It contains all clusters of richness class $R \geq 0$ with measured or estimated redshifts not exceeding $z_{lim} = 0.13$; beyond this limit the fraction of clusters with measured redshifts becomes small.

TABLE 1
Properties of the samples of X-ray clusters

Sample	N_{total}	Sky area	Energy band keV	CR_{limit} cts/s	Flux limit 10^{-12} ergs $\text{cm}^{-2}\text{s}^{-1}$	r_0 h^{-1} Mpc	γ
Ebeling 1998	201	$ b_g > 20^\circ, \delta > 0^\circ$	0.1 – 2.4		4.4	33.0	1.82
De Grandi 1999	130	$ b_g > 20^\circ, \delta < 2.5^\circ$	0.5 – 2.0		3 – 4	21.5	2.11
Schwope 2000	302	$ b_g > 30^\circ$	0.5 – 2.0	0.2	2.4	25	2.2

Note: for the correlation function parameters of the first two samples see Moscardini et al. 2000b and references therein

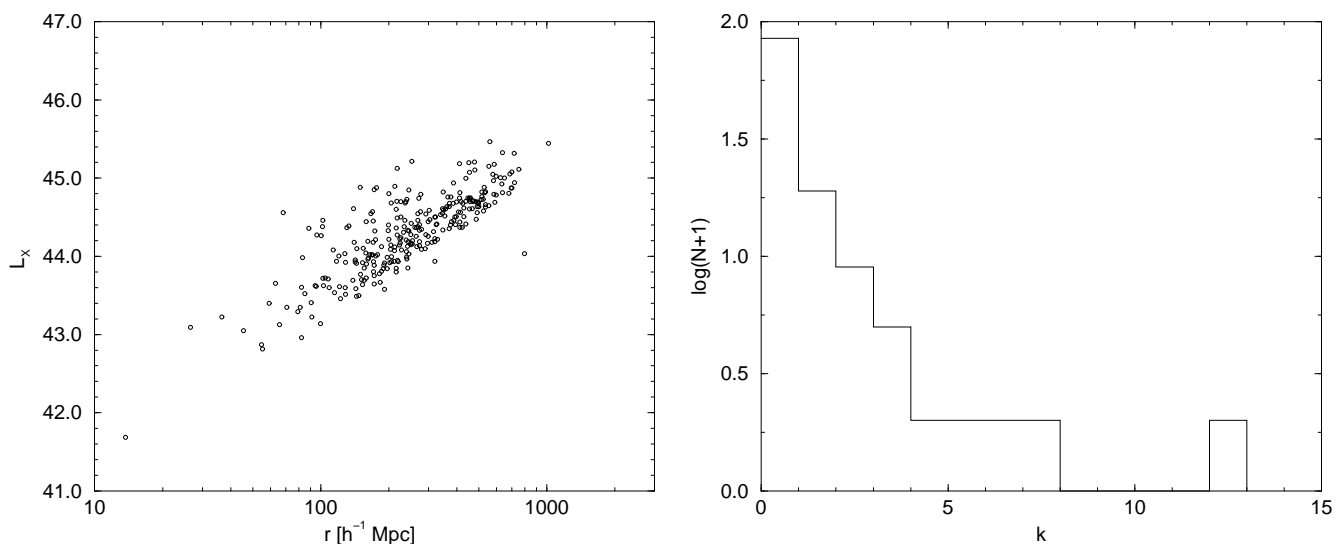


FIG. 2.— Left panel: the X-ray luminosity vs. distance for RBS clusters. Right panel: The number of X-ray clusters in superclusters of different multiplicity k ; isolated clusters are shown for comparison. System with the largest number of X-ray clusters is the Hercules supercluster

The sample contains 1662 clusters, 1071 of which have measured redshifts. We denote this sample of Abell clusters ACO.A1; A for all and 1 for lower limit of supercluster richness of clusters included into the sample. Einasto et al. (2001b, Paper III) present the correlation functions of Abell clusters for full samples (including clusters with estimated redshifts) and for samples which include only clusters with measured redshifts.

2.3. Superclusters of Abell and X-ray clusters

In our previous papers (e.g. E97d) we have shown that on large scales the correlation function characterizes the distribution of high-density regions. High-density regions are determined essentially by clusters of galaxies located in superclusters. We defined high-density regions, applying cluster analysis, as superclusters of Abell clusters, and as superclusters of X-ray clusters.

We searched for superclusters on the basis of both RBS.250 and Abell cluster samples using the friend-of-friend algorithm with a neighborhood radius of $24 h^{-1}$ Mpc; for details see Einasto et al. (1994, hereafter EETDA), Einasto et al. (1997d, hereafter E97d), Paper I and references therein. This radius was chosen according to the

clustering properties of Abell clusters: at this radius the friend-of-friend algorithm connects clusters into systems so that we obtain superclusters as the largest still relatively isolated systems. We applied the same neighborhood radius to the X-ray cluster sample and search for superclusters, i.e. systems of clusters with at least two members. A supercluster is called “rich” if it contains at least 4 member clusters, and “very rich” if it has at least 8 member clusters (E97d). The sample of Abell clusters which belong to the very rich superclusters is denoted as ACO.A8 (see Paper I for details and the list of superclusters based on Abell clusters).

In Figure 2 (right-hand panel) we show the number of systems of various richness in the RBS.250 sample for a neighborhood radius of $24 h^{-1}$ Mpc. In total there are 137 clusters in this sample. At this neighborhood radius about half of the X-ray clusters are still isolated, and there are only eight systems with four or more members. All these systems are embedded in superclusters previously determined from Abell clusters (E97d, Paper I). We denote the sample of superclusters found on the basis of RBS clusters as RBS.XSC.

Actually, a number of X-ray clusters that appear to be isolated in Figure 2 are members of superclusters of Abell

TABLE 2

Parameters of the selection function and the correlation function for various samples

Sample	$\sin b_0$	d_0 h^{-1} Mpc	p	N	r_0 h^{-1} Mpc	γ	P h^{-1} Mpc
RBS.250	0.22	100	1.0	137	24.7 ± 1.9	2.2 ± 0.3	115 ± 7
RBS.XSC	0.25	100	1.5	91	36.8 ± 2.1	2.4 ± 0.2	109 ± 19
RBS.A8	0.25	100	1.5	56	49.9 ± 6.3	2.2 ± 0.3	111 ± 18
ACO.A1	0.25	100	1.2	1662	17.6 ± 1.2	1.7 ± 0.2	113 ± 28
ACO.A8	0.40	100	1.0	373	36.7 ± 5.1	2.3 ± 0.4	115 ± 17

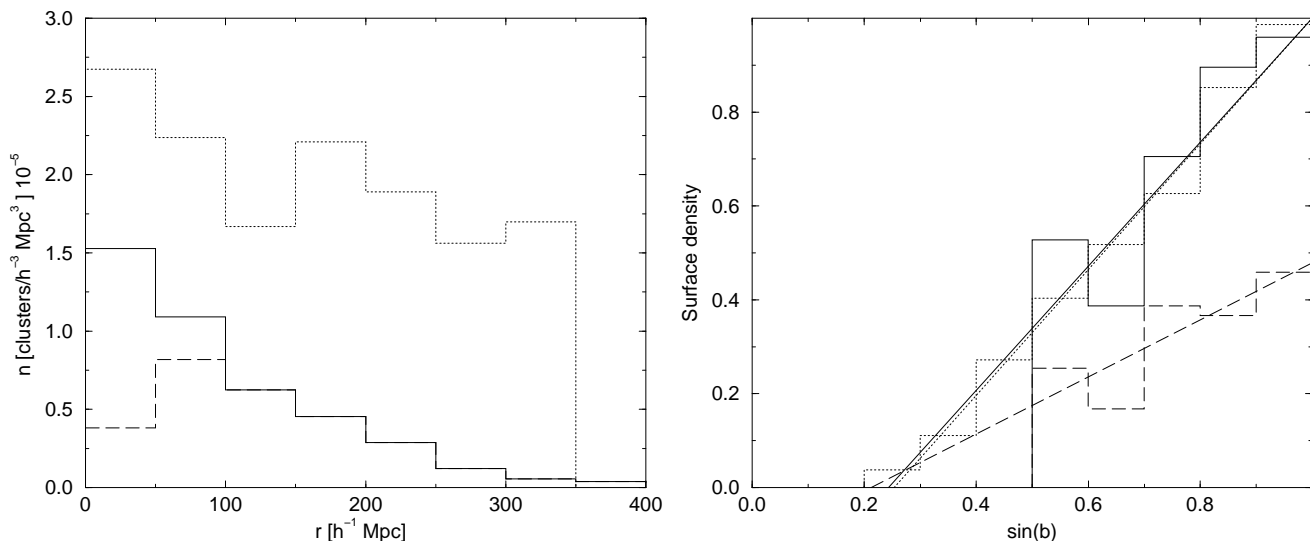
Note: in the last three columns 1σ errors are presented

FIG. 3.— Selection functions for X-ray and ACO clusters in distance (left-hand panel) and in Galactic latitude (right-hand panel). Dotted lines show selection function for the sample ACO.A1. Solid lines show the distribution of clusters in the whole sample RBS. Dashed lines show distribution of clusters in RBS.250 selected by limiting X-ray luminosity ($\log L_x > 43$, in both panels) and distance ($R < 250 h^{-1}$ Mpc, in the right-hand panel). In the right-hand panel the density is given in units of density at the Galactic pole (except for the RBS.250 which is scaled to the RBS density). Linear approximations are given for the respective latitude selection functions.

clusters. Thus it is necessary to determine X-ray clusters in superclusters also in another way: first we define superclusters on the basis of Abell clusters, and then find which superclusters contain X-ray clusters (for details and the lists of superclusters based on Abell X-ray clusters, and additional superclusters based on non-Abell X-ray clusters see Paper I). The sample of members of very rich superclusters among X-ray clusters obtained in this way is denoted as RBS.A8. The samples RBS.XSC and RBS.A8 are different. For example, if there is just one X-ray cluster among the members of a rich supercluster of Abell clusters then this cluster is included into sample RBS.A8, but not into sample RBS.XSC. On the other hand, if in a supercluster with four members all the members clusters are X-ray clusters then these clusters are included into sample RBS.XSC, but due to the richness limit they are not included into sample RBS.A8. In the following we show the correlation functions for both these samples, RBS.XSC and RBS.A8.

3. CORRELATION FUNCTION

3.1. Selection functions

Both the Abell and the X-ray cluster sample have a shape of a double-cone (with the observer at the tip of each cones). The X-ray cluster sample is bounded by Galactic latitude $|b_g| > 30^\circ$ and extends up to the distance of $250 h^{-1}$ Mpc. Even in this restricted volume the sample is not homogeneous in spatial density. To take into account selection effects in the X-ray samples we have determined galactic latitude and redshift selection functions. The procedure of finding of selection functions has been presented in detail in E97b, E97d, E99a.

Figure 3 shows selection functions for the X-ray (RBS) and Abell cluster based samples. The latitude selection can be represented by a linear dependence between surface number density S and $\sin b$

$$S(b) = (\sin b - \sin b_0)/(1 - \sin b_0), \quad (1)$$

where b_0 is a parameter in the linear regression. The distance dependence can be expressed as a power law

$$S(d) = \begin{cases} a_0, & d \leq d_0; \\ a_0(d_0/d)^p, & d > d_0; \end{cases} \quad (2)$$

here a_0 is the density of the sample near the observer, d_0 is the distance up to which redshift selection is considered constant, and p is the power law index. Parameters of the selection function for X-ray and Abell cluster samples are given in Table 2, where N is the number of clusters in a sample. The distance dependence shows that at the limiting distance of the sample RBS.250 ($250 h^{-1}$ Mpc) the density of the X-ray clusters is about 2.5 times lower than near the observer. These selection functions were taken into account in the calculation of the correlation functions for respective samples.

3.2. Correlation functions on large scales

Now we shall study the correlation function up to scales of $500 h^{-1}$ Mpc with the purpose to test the presence of oscillations found in correlation function of optically selected cluster samples. The problems which arise in connection with sample volume shape, selection functions, error estimates and sample dilution have been considered in detail in our earlier papers (E97b, E97d, E99a). The two-point spatial correlation function was calculated in the classical way using cluster pair separations :

$$\xi(r) = \frac{DD(r)}{RR(r)} - 1, \quad (3)$$

where $DD(r)$ is the number of pairs of clusters in the range of separations $r \pm dr/2$, dr is the bin size, $RR(r)$ is the respective number of pairs in a random sample scaled to the mean number density of clusters in the observed sample. It is assumed that both samples have identical shape, volume and selection functions. The mean error was calculated as given in E97b:

$$\sigma_\xi = \frac{b}{\sqrt{N}}, \quad (4)$$

where the value of the parameter b is ≈ 1.5 .

In Figure 4 we present the correlation function for the X-ray selected sample of clusters RBS.250 in comparison with correlation function of the optically selected (Abell) clusters sample ACO.A1. To decrease random sampling errors we applied Gaussian smoothing with a dispersion of $15 h^{-1}$ Mpc. Due to the smaller sample size of X-ray clusters the errors are larger than for the optically selected cluster sample (see E97d for a more detailed analysis of errors of a correlation function). The correlation function for X-ray selected clusters shows the oscillation with a period of about $115 h^{-1}$ Mpc as in the case of Abell clusters. Our earlier studies of optically selected clusters have shown (E97b) that correlation function of clusters belonging to high-density regions (i.e. superclusters) is oscillating with a higher amplitude than the correlation function of all clusters. In the lower panels of Figure 4 we present the correlation function of X-ray and Abell clusters which belong to superclusters as described in section 2.3 (samples RBS.A8, RBS.XSC and ACO.A8). We see that the amplitude of oscillations is really higher than for samples of all clusters. In

the left-hand panels we see five secondary maxima of the correlation function, in the right-hand panels (which cover a larger range of separations) even six. For the X-ray clusters which belong to rich superclusters the oscillations are more significant than for the sample of all X-ray clusters. Mean oscillation periods of the correlation function for each of our samples are presented in Table 2 (for details on the calculation of periods see E97b).

3.3. Correlation functions on small scales

The spatial correlation function of clusters of galaxies on small scales is usually expressed as a power law

$$\xi = (r/r_0)^{-\gamma}, \quad (5)$$

where r_0 is the correlation length, and γ the power index. In the left panel of Figure 5 we present the correlation function for all observed samples discussed in the present paper; in Table 2 we give correlation function parameters. We shall discuss our results in the last Section.

4. X-RAY CLUSTERS IN SUPERCLUSTERS AND THE $120 H^{-1}$ MPC SCALE

In previous Section we saw that the correlation functions for the X-ray cluster samples belonging to superclusters are oscillating at large separations with a period of about $115 h^{-1}$ Mpc. E97b and E97d demonstrated that oscillations of the correlation function at scales larger than $100 h^{-1}$ Mpc are caused by correlations between clusters in superclusters at opposite void walls, and appear only if superclusters form a quasi-regular network of step size which corresponds to the period of oscillations of the correlation function.

In order to understand better the behavior of the correlation function of X-ray clusters we shall study the distribution of superclusters of X-ray clusters. EETDA and E97d used various independent methods (void analysis, pencil-beam analysis, the nearest neighbor test) in addition to the correlation analysis to investigate the geometry of the supercluster-void network of Abell clusters. Due to the small number of X-ray clusters and superclusters we shall restrict our analysis to study of the distances between supercluster centers for rich superclusters of X-ray clusters. The distribution of these distances is given in the right-hand panel of Figure 5. We see several peaks in this distribution, at the distances of about 120, 190, 260 and $370 h^{-1}$ Mpc. We also calculated for each rich supercluster of X-ray clusters the distance to the nearest neighbor (distances between supercluster centers). This calculation shows that all rich superclusters of X-ray clusters have a neighboring rich supercluster at a distance interval of $100 - 135 h^{-1}$ Mpc. Thus peaks in Figure 5 correspond to the distances of the nearest system – step of the regularity, diagonal of the regularity and to two steps of the regularity. We see that direct calculations of distances between rich systems of X-ray clusters confirm the presence of the characteristic scale of $120 h^{-1}$ Mpc in the distribution of these clusters seen also in the correlation function.

We emphasize that the superclusters of X-ray clusters are all embedded in the superclusters of Abell clusters (see also Paper I), and both type of superclusters follow the same pattern of large-scale high-density regions in the Universe.

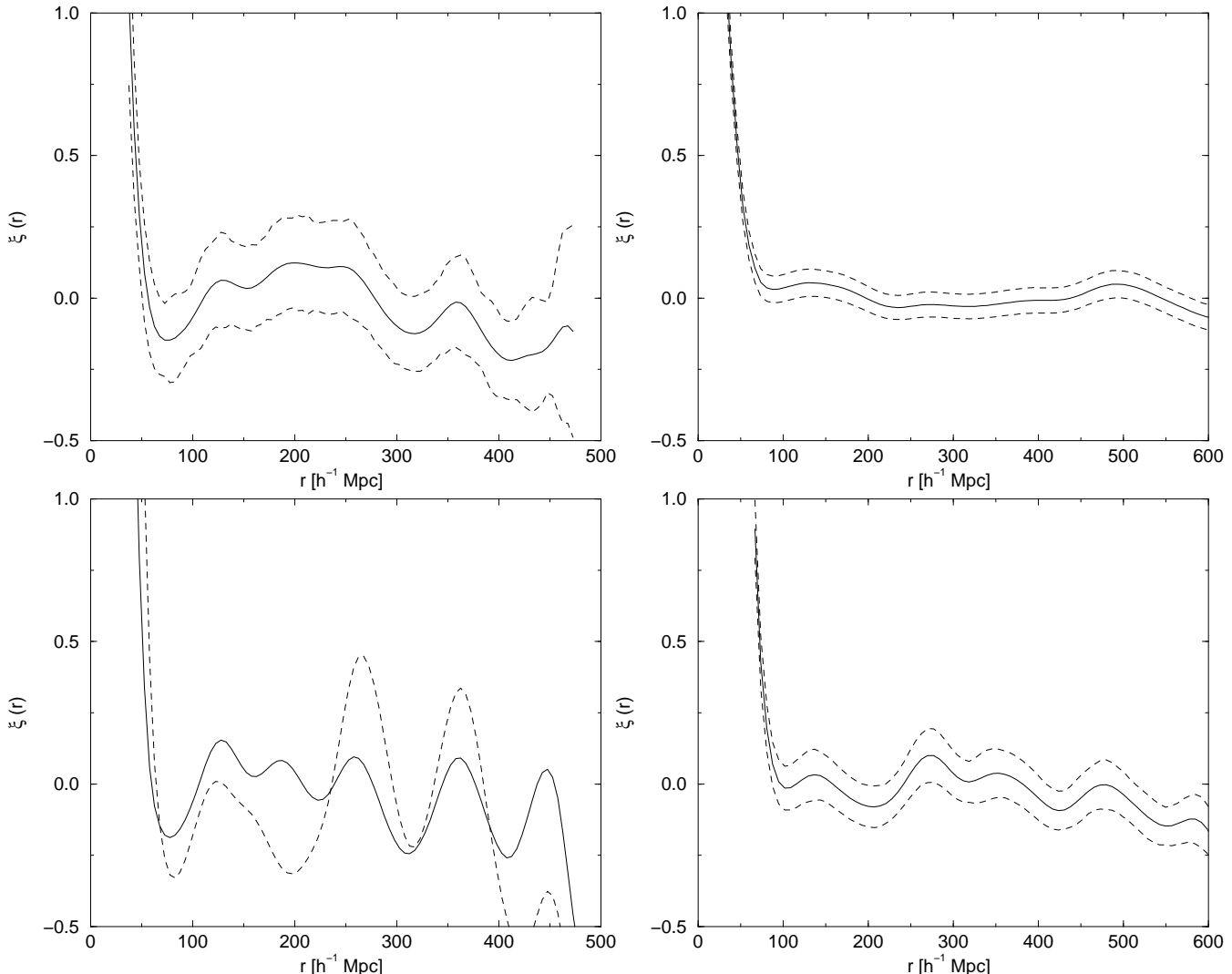


FIG. 4.— The correlation functions for X-ray clusters (left-hand panels) and optically selected Abell clusters (right-hand panels). Upper panels show correlation functions for the whole cluster samples RGB.250 and ACO.A1, the lower panels show clusters which belong to high density regions or superclusters (samples RBS.A8, RBS.XSC and ACO.A8). 3σ error corridors are shown with dashed lines. In the lower left panel the solid line is for X-ray clusters contained in X-ray superclusters (i.e. based on X-ray clusters only, $N_{Xcl} \geq 2$, sample RBS.XSC); the dashed line is based on the X-ray clusters in the rich Abell-cluster-based superclusters ($N_{Acl} \geq 8$, the sample RBS.A8).

The small number of X-ray clusters decreases the significance of this result if we consider X-ray clusters alone, but in combination with Abell cluster sample we can find main geometrical properties of the supercluster-void network.

In Figure 6 we plot the distribution of X-ray clusters in supergalactic coordinates; Abell clusters belonging to very rich superclusters are also shown. Filled symbols correspond to X-ray clusters in rich systems. We see that the distribution of X-ray clusters follows the supercluster-void network determined by Abell clusters (EETDA, E97d). We see a rather regular placement of rich systems that mainly determine the properties of the correlation function of X-ray clusters on large scales.

5. DISCUSSION AND CONCLUSIONS

It follows from the definition that the correlation function characterizes the distribution of pairs of clusters at different separations. Clusters form superclusters, thus we can say that on small scales the correlation functions describes the distribution of clusters within superclusters, and

on large scales the distribution of superclusters themselves. This property of the correlation function was discussed by Einasto et al. (1997c). Now we shall discuss in more detail how properties of superclusters and their distribution manifests itself in the correlations functions derived in the present paper.

First of all, we notice that different authors use slightly different algorithms to calculate the correlation function. Also the influence of various selection effects is treated differently. In Paper III we made an independent analysis of the correlation function of Abell clusters using a slightly different algorithm for the determination of the selection function. Thus it is appropriate to ask: Are our results compatible with results of previous investigators? So far the correlation function of clusters has been studied mostly up to a scale of $\sim 100 h^{-1}$ Mpc, and was characterized by parameters of the power law, the correlation length, r_0 , and the slope of the correlation function, γ . Values found in the present paper and given in Table 2 are in the range found previously (see, for example, Bahcall & West (1992),

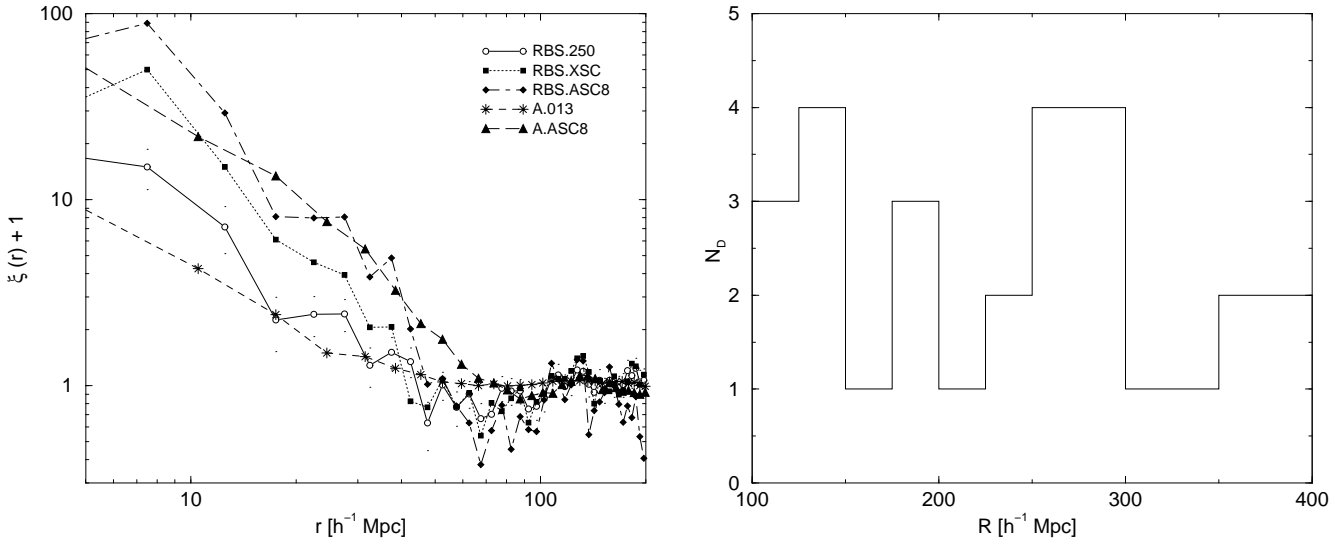


FIG. 5.— Left panel: correlation functions of Abell and X-ray selected clusters on a log-log scale; $\xi(r) + 1$ is given to present the correlation function at values $\xi \leq 0$. Right panel: histogram of distances between centers of rich superclusters of X-ray clusters.

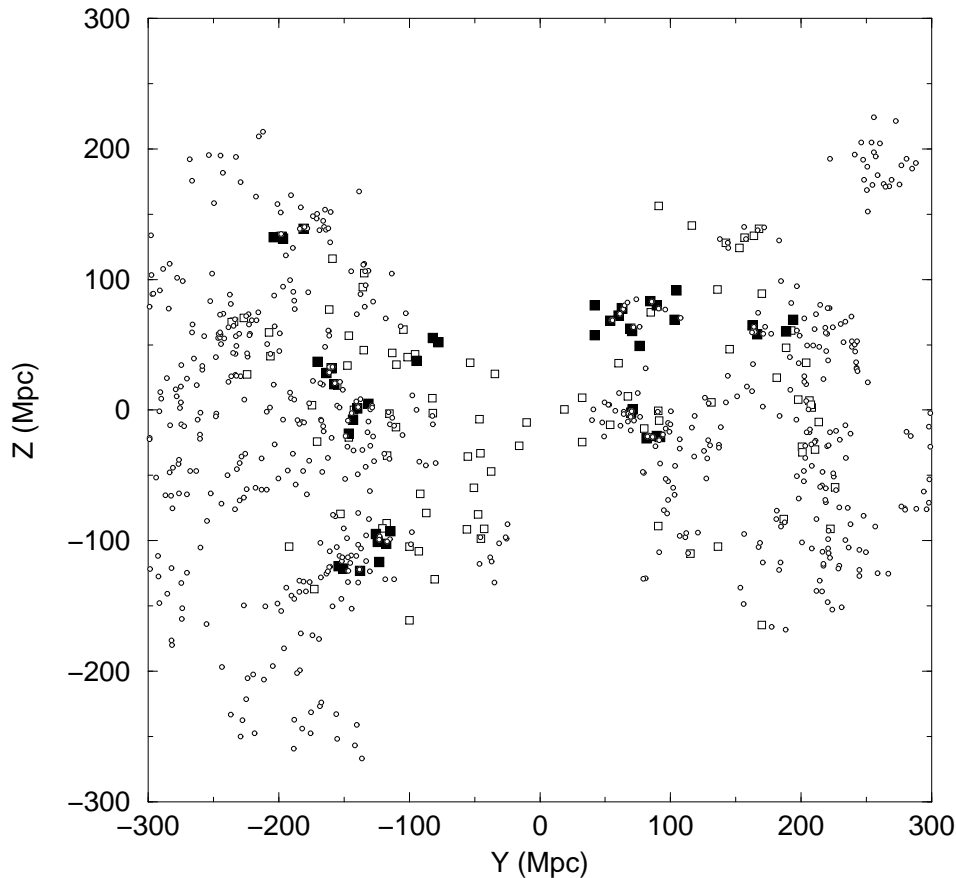


FIG. 6.— Distribution of X-ray and Abell clusters in supergalactic coordinates. Filled squares denote X-ray clusters in rich superclusters, open squares indicate isolated X-ray clusters and members of poor systems, while open circles mark Abell clusters. In order to minimize the projection effects we plot only member clusters of very rich superclusters with at least 8 members. The figure shows all clusters in the range $-300 h^{-1} \text{ Mpc} \leq \text{SGX} \leq +300 h^{-1} \text{ Mpc}$.

Croft et al. (1997), Guzzo et al. (1999), Lee & Park (1999), Moscardini et al. (2000), Collins et al. (2000)). Within the errors the correlation function parameters for Abell clusters coincide with values found in Paper III. The shape of the correlation function shown in Figure 5 (left-hand panel) is

also similar to the shape found previously by authors noted above. Thus we can say that our results are in qualitative agreement with previous studies; in other words, possible disturbing effects due to differences of the selection function and algorithms are not dominating our results.

Next we shall discuss differences of parameters of the correlation function found for different subsamples of Abell and X-ray selected clusters. The comparison of correlation functions presented in Figure 5 (left-hand panel) and parameter values given in Table 2 shows that the correlation functions of the Abell cluster full sample ACO.A1 and X-ray selected sample RBS.250 are rather similar. The X-ray sample has slightly higher correlation amplitude and steeper slope, but within random errors both values are within the range found earlier for different optically selected cluster samples. The correlation function of X-ray clusters in superclusters (sample RBS.XSC) has a higher amplitude and a larger correlation length. The highest amplitude and the largest correlation length are obtained for samples of clusters in very rich superclusters, RBS.A8 and ACO.A8. Among these two the X-ray selected sample has a higher amplitude.

These results can be understood as the effect of different threshold density used in the definition of clusters in superclusters of different richness, or, in other words, due to different bias levels of samples. This aspect has been studied in detail by Einasto et al. (1999b). Galaxy and cluster samples are defined by the density field of matter using various threshold densities to exclude objects located in a low-density environment. In galaxy samples the matter in voids has been excluded, in cluster samples not only the matter in voids but also the matter in low-density filaments is excluded from the analysis. Clusters in superclusters and very rich superclusters correspond to an increasingly higher density cut-off. As demonstrated by Einasto et al. (1999b), a higher density cut-off rises the amplitude of density fluctuations of objects selected through such a procedure. This biasing phenomenon is well known since the pioneering work by Kaiser (1984).

Now we consider the correlation function on large scales. As noted above, on large scales the correlation function describes the distribution of superclusters. If superclusters are randomly distributed, then the correlation function is approximately equal to zero for large separations. On the other hand, if superclusters form a regular lattice, then the correlation function oscillates with a period equal to the step size of the lattice (see Einasto et al. 1997c for a detailed analysis). We notice that the correlation functions of all cluster samples have a negative section around $r \approx 80 h^{-1}$ Mpc and a secondary maximum on scales of $r \approx 130 h^{-1}$ Mpc. This negative section followed by a secondary maximum is a clear indication for the presence of a dominating scale in the distribution of superclusters, even if there is no large-scale regularity in the distribution of superclusters; an example is the Voronoi tessellation model (Einasto et al. 1997c). Our cluster samples, both optically and X-ray selected, have not only this property but show a clear signature of oscillations with a period $\sim 120 h^{-1}$ Mpc. The amplitude of oscillations of X-ray selected clusters is higher than the amplitude for optically selected Abell clusters in superclusters of similar richness. This property shows that cluster samples have not only a scale but also a regularity in their distribution. This feature is stronger in X-ray selected cluster samples, in other words, X-ray clusters are even better indicators for the lo-

cation of high-density regions in the Universe. It is interesting to note that in Paper I we reached the same conclusion from an analysis of supercluster memberships: the fraction of isolated X-ray clusters is smaller than the fraction of isolated Abell clusters, and the fraction of X-ray clusters in rich superclusters is higher than in poor superclusters. This is also an evidence that X-ray clusters are better tracers of the supercluster-void network than optical clusters. Some other studies have also shown the presence of a scale of $\sim 120 h^{-1}$ Mpc in the distribution of high-density regions in the Universe (Broadhurst et al. 1990, E97b, E97d, Broadhurst & Jaffe 1999, Guzzo 1999).

The present study gives no answer to the question: Is the presence of a scale in the distribution of rich superclusters and their regular displacement a local or a global phenomenon in the Universe? Larger samples of X-ray clusters which shall be available in the near future shall reveal the distribution of X-ray clusters in a larger volume and shall yield a better information on the distribution of high-density regions in the Universe.

To summarize our discussion we can say the following.

- 1) The correlation analysis has confirmed that both the optically selected Abell sample and the X-ray selected RBS sample trace high-density regions in the Universe in a similar fashion.
- 2) Correlation properties of cluster samples depend on the environment of clusters: clusters in rich superclusters (high local density) have a larger correlation length and amplitude; there exists no unique value of the correlation length of clusters of galaxies.
- 3) On large scales the correlation function of clusters depends on the distribution of superclusters. Both optically and X-ray selected cluster samples have an oscillating correlation function with alternating maxima and minima. The period of oscillations is $\sim 115 h^{-1}$ Mpc. The amplitude of oscillations is larger in superclusters of higher richness; for superclusters of similar richness the amplitude of oscillations in X-ray selected cluster samples is higher than in samples of optically selected clusters.
- 4) The effective volume covered by the RBS sample is smaller than the volume covered by the Abell sample, and the number of known clusters is smaller. The RBS sample is the largest (in volume) X-ray selected sample available. Quantitative statistics based on X-ray selected clusters have still a lower significance than those based on optically selected samples. Due to small volume X-ray selected samples cannot be considered as fair samples of the Universe.
- 5) In combination, optical and X-ray selected samples enhance results obtained separately.

We thank Günther Hasinger for providing us with a draft version of the RBS catalog and discussion of preliminary results of the study, and Jaak Jaaniste, Enn Saar, Jaan Pelt and Alexei Starobinsky for stimulating discussion. This work was supported by Estonian Science Foundation grant 2625. JE thanks Astrophysical Institute Potsdam for hospitality where part of this study was performed. HA thanks CONACyT for financial support under grant 27602-E.

REFERENCES

- Abadi, M.G., Lambas, D.G., & Muriel, H. 1998, ApJ, 507, 526
- Abell, G. 1958, ApJS, 3, 211
- Abell, G., Corwin, H., & Olowin, R. 1989, ApJS, 70, 1 (ACO)
- Andernach, H., & Tago, E. 1998, In: Proc. "Large Scale Structure: Tracks and Traces", eds. V. Müller, S. Gottlöber, J.P. Mücke, & J. Wambsganss, World Scientific, Singapore, p. 147
- Bahcall, N.A., & West, M.J. 1992, ApJ, 392, 419
- Broadhurst, T.J., Ellis, R.S., Koo, D.C., & Szalay, A.S. 1990, Nature, 343, 726
- Broadhurst, T.J., & Jaffe, A.H. 1999, ApJ, submitted [astro-ph/9904348]
- Collins, C.A., Guzzo, L., Böhringer, H., Schuecker, P., Chincarini, G., Cruddace, R., De Grandi, S., MacGillivray, H.T., Neumann, D.M., Schindler, S., Shaver, P., & Voges, W. 2000, MNRAS, 319, 939
- Croft, R.A.C., Dalton, G.B., Efstathiou, G., Sutherland, W.J., & Maddox, S.J. 1997, MNRAS, 291, 305
- De Grandi, S., Böhringer, H., Guzzo, L., Molendi, S., Chincarini, G., Collins, C., Cruddace, R., Neumann, D., Schindler, S., Schuecker, P., & Voges, W. 1999, ApJ, 514, 148
- Ebeling, H., Edge, A., Böhringer, H., Allen, S.W., Crawford, C.S., Fabian, A.C., Voges, W., & Huchra, J.P. 1998, MNRAS, 301, 881
- Ebeling, H., Edge, A., Allen, S.W., Crawford, C.S., Fabian, A.C., & Huchra, J.P. 2000, MNRAS, submitted [astro-ph/0003191]
- Einasto, J., Einasto, M., Gottlöber, S., Müller, V., Saar, V., Starobinsky, A.A., Tago, E., Tucker, D., Andernach, H., & Frisch, P. 1997a, Nature, 385, 139
- Einasto, J., Einasto, M., Frisch, P., Gottlöber, S., Müller, V., Saar, V., Starobinsky, A.A., Tago, E., Tucker, D., & Andernach, H. 1997b, MNRAS, 289, 801 (E97b)
- Einasto, J., Einasto, M., Frisch, P., Gottlöber, S., Müller, V., Saar, V., Starobinsky, A.A., & Tucker, D., 1997c, MNRAS 289, 813
- Einasto, J., Einasto, M., Tago, E., Starobinsky, A.A., Atrio-Barandela, F., Müller, V., Knebe, A., Frisch, P., Cen, R., Andernach, H., & Tucker D. 1999a, ApJ, 519, 441 (E99a)
- Einasto, J., Einasto, M., Tago, E., Müller, V., Knebe, A., Cen, R., Starobinsky, A.A. & Atrio-Barandela, F., 1999b, ApJ 519, 456
- Einasto M., Einasto J., Tago, E., Dalton, G., & Andernach, H. 1994, MNRAS, 269, 301 (EETDA)
- Einasto, M., Tago, E., Jaaniste, J., Einasto, J., & Andernach, H. 1997d, A&A Suppl., 123, 119 (E97d).
- Einasto, M., Einasto, J., Tago, E., Hasinger, G., Müller, V., & Andernach, H. 2001a, AJ, submitted (Paper I)
- Einasto, M., Einasto, J., Tago, E., Andernach, H., Dalton, G.B., & Müller, V., 2001b, AJ, submitted (Paper III)
- Guzzo, L. 1999, invited review at the 19th Texas Symposium on Relativistic Astrophysics, Paris, Dec. 1998 [astro-ph/9911115]
- Guzzo, L., Böhringer, H., Schuecker, P., Collins, C.A., Schindler, S., Neumann, D.M., De Grandi, S., Cruddace, R., Chincarini, G., Edge, A., Shaver, P., & Voges, W. 1999, Messenger 95, 27
- Kaiser, N. 1984, ApJ, 284, L9
- Lee, S., & Park, C. 1999, ApJ, submitted [astro-ph/9909008].
- Mattig, W. 1958, Astr. Nachr. 284, 109
- Miller, C., & Batuski, D. 2000, ApJ, submitted [astro-ph/0002295]
- Moscardini, L., Matarrese, S., De Grandi, S., & Lucchin, F.P. 2000a, MNRAS, 314, 647
- Moscardini, L., Matarrese, & H.J.Mo 2000b, submitted to MNRAS, [astro-ph/0009006]
- Peacock, J.A., & Dodds, S.J. 1994, MNRAS, 267, 1020
- Retzlaff, J., Borgani, S., Gottlöber, S., Klypin, A., & Müller, V. 1998, NewA, 3, 631
- Retzlaff, J. 1999, MPE Report, 271, 177
- Romer, A.K., Collins, C., Böhringer, H., Cruddace, R., Ebeling, H., MacGillivray, H.T., & Voges, W. 1994, Nature, 372, 75
- Schwope, A.D., Hasinger, G., Lehmann, I., Schwarz, R., Brunner, H., Neizvestny, S., Ugryumov, A., Balega, Yu., Trümper, J., & Voges, W. 2000, Astron. Nachr., 321, 1
- Schuecker, P., Böhringer, H., Guzzo, L., Collins, C.A., Neumann, D.M., Schindler, S., Voges, W., De Grandi, S., Chincarini, G., Cruddace, R., Müller, V., Reiprich, T.H., Retzlaff, J., & Shaver, P. 2000, A&A, submitted, [astro-ph/0012105]
- Tesch, F., Carrera, F. J., Engels, D., Hu, J., Ledoux, C., Ugryumov, A., Valls-Gabaud, D., Voges, W., & Wei, J. 2000, in "Large Scale Structure in the X-ray Universe, eds. M. Plionis, & I. Georgantopoulos, Atlantisciences, Paris, France, p. 407
- Vogele, M. 1998, *The Evolving Universe*, ed. D. Hamilton, (Dordrecht: Kluwer), p. 395 [astro-ph/9805160]
- Voges, W., Aschenbach, B., Boller, T., et al., 1999, A&A 349, 389